Machine learning for comprehensive prediction of high risk for Alzheimer's Disease based on chromatic pupilloperimetry

Yael Lustig-Barzelay
Goldschleger Eye Research Institute, Sheba Medical Center
Ifat Sher
Goldschleger Eye Research Institute, Sheba Medical Center
Inbal Sharvit-Ginon
The Joseph Sagol Neuroscience Center, Sheba Medical Center, Tel Hashomer
Yael Feldman
Goldschleger Eye Research Institute, Sheba Medical Center
Michael Mrejen
Condensed Matter Physics Department, School of Physics and Astronomy, Tel-Aviv University
Abigail Livny
Department of Diagnostic imaging, Sheba Medical Center, Tel Hashomer
Michal Schnaider-Beeri
The Joseph Sagol Neuroscience Center, Sheba Medical Center, Tel Hashomer
Aron Weller
Gonda Brain Research Center, Bar Ilan University
Ramit Ravona-Springer
The Joseph Sagol Neuroscience Center, Sheba Medical Center, Tel Hashomer
Ygal Rotenstreich (Ygal.Rotenstreich@sheba.health.gov.il)
Goldschleger Eye Research Institute, Sheba Medical Center

Research Article

Keywords:

Posted Date: February 15th, 2022

DOI: https://doi.org/10.21203/rs.3.rs-1317181/v1

Abstract

Currently there are no reliable biomarkers for early detection of Alzheimer's disease (AD) at the preclinical stage. This study assessed the pupil light reflex (PLR) for focal red and blue stimuli in central and peripheral retina in 125 cognitively normal middle age subjects (45-71 YO) at high risk for AD due to a family history of the disease, and 61 age-similar subjects with no family history of AD using Chromatic Pupilloperimetry coupled with Machine Learning (ML). All subjects had normal ophthalmic assessment, and normal retinal and optic nerve thickness by optical coherence tomography. No significant differences were observed between groups in cognitive function and volumetric brain MRI. Chromatic pupilloperimetry-based ML models were highly discriminative in differentiating subjects with and without AD family history, using transient PLR for focal red (primarily cone-mediated), and dim blue (primarily rod-mediated) light stimuli. Features associated with transient PLR latency achieved Area Under the Receiver Operating Characteristic Curve of 0.90 ± 0.051 (left-eye) and 0.87 ± 0.048 (right-eye). Parameters associated with the contraction arm of the rod and cone-mediated PLR were more discriminative compared to parameters associated with the relaxation arm and melanopsin-mediated PLR. Taken together our study suggests that subtle focal changes in pupil contraction latency may be detected decades before the onset of AD clinical symptoms. The dendrites of melanopsin containing retinal ganglion cells may be affected very early at the preclinical stages of AD.

Introduction

Over 35 million people world-wide live with Alzheimer's Disease (AD), the most common form of dementia [1]. Treatments have limited effects on symptoms, and while the FDA recently approved a drug that targets successfully the pathology of AD [2], there is no sufficient evidence supporting cognitive benefits. The lack of cognitive benefits may be attributed, among other factors, to the introduction of treatment at the clinical phases of the disease, when the brain is overwhelmed by pathology, which begins decades before the clinical symptoms become explicit. Early detection of AD, at the pre-clinical stage, or identification of patients at risk, is critical for implementing preventative measurements, and for effective clinical trials of disease modifying treatments[3,4]. First degree family history of AD was found to be a major risk factor for developing the disease [5–9]. However currently there are no clinical tests that can predict AD development.

The retina is considered an accessible extension of the central nerve system. As such, previous studies investigated whether retinal and optic nerve structural changes can be identified at pre-clinical stages of AD, with results remaining inconclusive [10–12]. The Pupillary Light Reflex (PLR) is mediated by intrinsically photosensitive retinal ganglion cells (ipRGC) that receive internal inputs from intrinsic activation of melanopsin, and external inputs from the outer retinal photoreceptors, namely the rods and the cones. The ipRGCs mediate the PLR and the light entrainment of the circadian rhythm. Recent studies demonstrated abnormal circadian function and loss of ipRGCs in post-mortem eyes of AD patients [13]. Pupillometry is a simple, fast, and non-invasive test that is gaining interest as a potential readily accessible tool for assessment of neurodegenerative processes in the retina and the brain[14,15]. Several

studies indicated changes in the PLR in response to white light stimuli in AD patients, yet the results remain inconclusive, most likely due to differences in methodologies (reviewed in [15]). Thus, some studies indicated reduced baseline pupil diameter in AD patients compared with controls [16–18], whereas others reported insignificant differences in baseline pupil size [19,20]. Several studies demonstrated increased contraction latency, decreased contraction amplitude and reduced mean contraction velocity [17,19–23]. Differences in re-dilation phase after light offset were also reported [16,17] and pupil recovery time was found to be longer in autosomal dominant AD mutation carriers [24]. Finally, two studies reported that Mini Mental State Examination (MMSE) and Wechsler memory scores in AD patients correlated moderately with acceleration, velocity and latency of pupil contraction [25,19]. However, another study that compared between the PLR of pre-clinical AD patients and healthy controls, using flashes of white light, found no differences in the contraction and re-dilation phases [26].

Chromatic pupillometry enables the assessment of the relative contribution of cones, rods, and melanopsin to the PLR by measuring the PLR for red, dim and bright blue, light stimuli, respectively[27–31] .Pupillometry studies using full-field (>90 degree) blue and red-light stimuli reported contradictory results. Thus, Oh et al reported no difference between the PLR recorded in 10 subjects over 60 years old at high risk to develop AD, based on abnormal values of cerebrospinal fluid (CSF) amyloid β_{1-42} and total Tau protein [32]. By contrast, Romagnoli et al reported attenuated rod mediated PLR, in 26 mild-moderate AD patients (mean age 69.3 years old) compared to age similar controls [33]. Since large (>90 degree) light stimuli were used in those studies, the PLR recorded reflected the mean response of ipRGCs across the retina, masking possible focal changes in intrinsic and extrinsic activation of ipRGCs [31,34] .

Chromatic pupilloperimetry measures the PLR for 54 small (0.43°) dim and bright red and blue light stimuli presented at a 30-degree visual field, thereby allowing examination of the rod-, cone- and melanopsin mediated-PLR at various retinal locations. Previous studies indicated the feasibility of detecting focal changes in retinal function in patients with retinal and macular degeneration by utilizing chromatic pupilloperimetry with high sensitivity and specificity[34–37]. Those studies indicated that the transient PLR obtained in response to short (1 sec) focal low intensity (dim) blue light stimuli is mainly mediated by rod photoreceptors, and cone photoreceptors significantly contribute to the PLR for focal red light stimuli [34–38]. Melanopsin-contribution to the PLR can be assessed by presenting bright blue light stimuli [31]. In this study, we combined the use of chromatic pupilloperimetry, with machine learning-based analysis, and demonstrated a potential novel approach for identifying the existence of a high risk for developing AD, in a large cohort (n=186) of cognitively asymptomatic middle-aged subjects based on the PLR for focal chromatic light stimuli.

Results

Demographic and cognitive features analysis

One hundred and eighty-six IRAP participants [mean age 59.7 (SD = 6.37) and 64.5% (n = 120) women] were included in the analysis. Of these, 125 (67.2%) were FH+, and 61 (32.8%) were FH−. Participant's age span was 44 – 71 years old (YO) and there was no significant difference in age between groups (Table 1). However, FH- participants had more years of education (p=0.0216). The proportion of women in the IRAP study was higher than men, especially in the FH- group. No significant differences in total gray matter and hippocampal volumes were observed between groups after adjustment for total intracranial volume (Table 1).

Table 1
Descriptive characteristics of the study cohort by Alzheimer Disease (AD) family history

	FH+*	**FH-***	**p-value**
Demographic characteristics			
N	125	61	
Age mean (SD) [#]	59.93 (± 6.69)	59.08 (± 5.56)	0.385
Female participants	75 (60%)	45 (74%)	0.065
Education years	15.84 (± 3.30)	17.03 (± 3.26)	**0.022**
Brain MRI-volumetric			
N	97	30	
Gray matter[$], Mean (SD)	587.8 (53.39)	568.8 (51.3)	0.317
Hippocampus[$], Mean (SD)	0.322 (0.032)	0.317 (0.033)	0.792
*FH=Family history of AD; [#]Age=Age at pupilloperimetry testing; [$] SD=standard deviation; [$] Mean of total volumes in cubic centimeters			

In an unadjusted analysis, FH+ cognitive performance was comparable to the performance FH- in the three cognitive domains. No significant differences in cognitive scores were observed between groups after adjustment for age, sex, and education (Supplementary Table 1).

Machine learning models

The AUC-ROC curve for each one of our 136 trained models is presented in Table 2 and Supplementary Table 2. The models that achieved the highest discriminative performances were the latency of the transient pupil contraction from light onset in response to dim blue (B_PRL) and red (R_PRL) light (Figure 1). The AUC-ROC values of these two parameters were 0.90 ± 0.051, CI of [0.81, 0.98] (left eye), 0.87 ± 0.048, CI of [0.77, 0.95] (right eye) in response to blue light and of 0.85 ± 0.05, CI of [0.75, 0.93] (left eye), 0.81 ± 0.06, CI of [0.68, 0.91] (right eye) in response to red light.

Table 2
Performance values of all classification models based on single PLR parameters in response to illumination with dim blue and red light.

		Left Eye		Right Eye	
PLR parameter		AUC-ROC 95% CI	AUC-ROC: Mean ± std	AUC-ROC 95% CI	AUC-ROC: Mean ± std
Dim blue	AC	[0.41,0.68]	0.548±0.069	[0.34,0.60]	0.473 ± 0.065
	LMCA	[0.66,0.90]	0.790±0.061	[0.60,0.85]	0.728 ± 0.065
	LMCD	[0.68,0.91]	0.809±0.058	[0.63,0.87]	0.756 ± 0.063
	LMCV	[0.35,0.62]	0.491±0.070	[0.35,0.63]	0.491 ± 0.070
	LMP	[0.54,0.81]	0.682±0.069	[0.55,0.82]	0.702 ± 0.068
	LMRA	[0.49,0.76]	0.627±0.069	[0.45,0.71]	0.586 ± 0.068
	LMRD	[0.48,0.76]	0.626±0.072	[0.46,0.72]	0.596 ± 0.068
	LMRV	[0.41,0.69]	0.558±0.070	[0.37,0.63]	0.505 ± 0.067
	MCA	[0.35,0.61]	0.483±0.067	[0.34,0.60]	0.471 ± 0.065
	MCD	[0.37,0.62]	0.495±0.065	[0.36,0.63]	0.506 ± 0.071
	MCV	[0.39,0.65]	0.525±0.065	[0.32,0.58]	0.451 ± 0.066
	MRA	[0.39,0.65]	0.520±0.066	[0.40,0.68]	0.543 ± 0.069
	MRD	[0.42,0.70]	0.567±0.070	[0.36,0.63]	0.493 ± 0.069
	MRV	[0.36,0.62]	0.490±0.066	[0.33,0.59]	0.466 ± 0.067
	PPC	[0.41,0.68]	0.549±0.067	[0.35,0.62]	0.486 ± 0.069
	PRL	[0.79,0.98]	0.903±0.051	[0.77,0.95]	0.873 ± 0.048
	PRP	[0.36,0.64]	0.502±0.070	[0.36,0.63]	0.500 ± 0.068
Dim Red	AC	[0.36,0.63]	0.489±0.068	[0.38,0.65]	0.519 ± 0.067
	LMCA	[0.61,0.84]	0.735±0.061	[0.54,0.80]	0.683 ± 0.067
	LMCD	[0.65,0.89]	0.782±0.060	[0.58,0.84]	0.720 ± 0.065
	LMCV	[0.34,0.59]	0.466±0.065	[0.36,0.62]	0.490 ± 0.066
	LMP	[0.49,0.77]	0.639±0.072	[0.63,0.90]	0.782 ± 0.072

Data are resented as the Confidence Interval (CI), Mean ± Standard Deviation (STD) and AUC-ROC, using 2000 iterations, for each one of 68 trained models. Each row indicates one PLR parameter. Each parameter appears twice, induced by dim blue and red light.

	Left Eye		Right Eye	
LMRA	[0.49,0.76]	0.639±0.068	[0.44,0.71]	0.585 ± 0.068
LMRD	[0.49,0.76]	0.635±0.069	[0.41,0.69]	0.553 ± 0.069
LMRV	[0.35,0.62]	0.488±0.069	[0.38,0.65]	0.522 ± 0.070
MCA	[0.37,0.64]	0.510±0.068	[0.36,0.63]	0.497 ± 0.068
MCD	[0.39,0.65]	0.526±0.068	[0.38,0.65]	0.517 ± 0.066
MCV	[0.41,0.69]	0.564±0.072	[0.37,0.62]	0.497 ± 0.068
MRA	[0.37,0.63]	0.501±0.065	[0.39,0.67]	0.531 ± 0.073
MRD	[0.40,0.67]	0.540±0.070	[0.35,0.61]	0.482 ± 0.065
MRV	[0.33,0.59]	0.462±0.065	[0.36,0.62]	0.489 ± 0.066
PPC	[0.35,0.61]	0.478±0.065	[0.37,0.63]	0.501 ± 0.067
PRL	[0.41,0.70]	0.556±0.075	[0.40,0.67]	0.536 ± 0.068
PRP	[0.73,0.95]	0.852±0.056	[0.69,0.90]	0.813 ± 0.056

Data are resented as the Confidence Interval (CI), Mean ± Standard Deviation (STD) and AUC-ROC, using 2000 iterations, for each one of 68 trained models. Each row indicates one PLR parameter. Each parameter appears twice, induced by dim blue and red light.

Other models that achieved acceptable discriminative values (AUC≥0.7) for both eyes were those related to latency of acceleration and deceleration of pupil contraction for dim red and blue light: *B_LMCA, R_LMCA, B_LMCD and R_LMCD*. The parameters *B_LMP* and *R_LMP*, (the latency of maximal pupil contraction from light onset), achieved high discriminative values for the right eye but low values for the left eye. The remaining parameters related to the latency of pupil contraction for dim blue and red light (*B_LMCV* and *R_LMCV)*, which measure latency of maximal velocity, gave AUC-ROC < 0.7 (Figure 1). All models derived from PLR for bright red or blue light stimuli gave very low AUC-ROCs (≤0.45) resembling random classification (Supplementary Table 2).

Focal analysis

Figure 2 presents the two most prominent parameters (*PRL for dim blue and red light stimuli*) and the weights given by the machine-learning model to each one of the 54 test- targets measured. Overall, the test targets most discriminative of a positive AD family history in response to dim blue light were located in the periphery of the 24-degree visual field, particularly in the temporal side (nasal side of the retina). In response to dim red light stimuli, discriminative test targets were detected throughout the retina with no specific pattern.

Discussion

Using chromatic pupilloperimetry testing in conjunction with machine learning algorithms we demonstrated that multi-parametric analysis of PLR kinetics for focal red and blue light stimuli can differentiate with high discriminative power cognitively asymptomatic individuals at high risk for AD due to a parental family history from individuals with no family history of AD.

The main contributions of this study are two; First, our prediction model could classify normally cognitively asymptomatic individuals according to the existence of AD family history, which is a major risk factor for developing the disease. Second, the prediction model achieving highest AUC-ROC was based on parameters pertaining to the latency of the transient PLR contraction phase. Our findings are supported by studies demonstrating changes in AD patients compared to healthy controls in PLR parameters related to the afferent arm of the reflex. Among them, some studies reported changes in latency-related PLR parameters [21,22], while others found changes in PLR parameters pertaining to the contraction phase, but not to the latency of the response [16,17,23]. To the best of our knowledge this is the first study that shows an association of attenuation of the afferent PLR arm with AD risk due to a parental family history in asymptomatic middle-aged adults. Our machine learning algorithm may detect changes in PLR in individuals at high risk for AD, years before the onset of cognitive decline.

The PLR parameter that achieved the highest performance rates by our learning algorithm for both eyes was the latency of the transient PLR, suggesting an effect on the contraction arm of the PLR, which is attributed to parasympathetic system. This finding is supported by studies demonstrating that AD Patients have reduced synthesis of Acetylcholine [39], the key neurotransmitter in the para-sympathetic nervous system [40]. AD affects the cholinergic system [41], and specifically the cholinergic Edinger Westphal Nucleus (EWN), [42,43] which is involved in the control of the pupil contraction [44]. Our findings are in accordance with published studies with patients with probable AD reporting attenuated pupil contraction acceleration [22,45,46], shorter PLR latency and lower amplitude of pupil contraction [45].

Using the pupil response latency (PRL) parameter, the highest performance values were obtained for both eyes were in response to dim blue light with lower, yet still very high performance for red light. These results demonstrate a slightly higher performance for the blue light illumination indicating that attenuation of the rod PLR pathway may be a very early event in the pre-AD stage. Interestingly, the most discriminative test targets of a positive AD family history in response to dim blue light were located in periphery of the visual field, in the temporal area, whereas in response to dim red light stimuli, discriminative test targets were detected across the visual field with no specific pattern. These finding may suggest attenuated function of the neuronal circuits downstream of rods in the nasal retina in early stages of AD pathogenesis. Furthermore, these findings indicate the possibility of running a shorter chromatic pupilloperimetry test, using a smaller number of test targets spots in the temporal visual field, that may suffice for screening using such classification algorithm. This should be validated in further studies. Differences in rod pathway function were also observed in full-field electrophysiology studies in mouse models of AD, where abnormal dark adapted retinal function was recorded, whereas cone photoreceptor function and signal transmission to second order neurons was maintained [47,48].

Since the PLR for bright red and blue light had low discrimination between groups, our data suggest that at the early pre-AD stage, the extrinsic ipRGC activation is affected whereas the melanopsin-mediated intrinsic activation of ipRGCs remains intact. Our findings are in accordance with the finding of Romagnoli et al who reported similar melanopsin-mediated but aberrant rod-mediated PLR in mild-moderate AD patients using full-field chromatic pupillometry [33]. Moreover, a recent pathology postmortem study indicated significant thinning of ipRGC dendrites in retinas of AD patients[13], providing a structural support for our functional findings.

All parameters with AUC-ROC > 0.7 were related to PLR latency suggesting a possible attenuation of the speed of neuronal signaling associated with high risk of AD disease. The only latency-related parameter that had AUC-ROC <0.7 for both eyes was the latency of maximal velocity (LMCV). Several studies indicated that the LMCV parameter differentiates with high specificity and sensitivity between healthy controls and patients with photoreceptor degeneration[35,37]. SD-OCT imaging for all participants included in the current study did not indicate any sign of photoreceptor degeneration. Hence, our findings that the LMCV did not change in response to either red or blue light, while other latency parameters differentiated between the study groups, suggest that the PLR pathology at the pre-clinical stage of AD does not occur at the photoreceptor cell level but rather downstream at the bipolar/amacrine or ipRGC dendrites. These findings are in accordance with the findings of McAnany et al., who have most recently reported post-receptor abnormalities in retinal function in a mouse model of AD under dark adaptation using fill field ERG [47].

Our study has several limitations. First, our cohort included 186 participants. Since each participant had PLR examinations done on both eyes, we ran our experiments on two datasets, a dataset for the left eye and for the right eye, with each dataset consisting of data extracted from 372 eyes. Although our data set was rather large, verification of the results in larger cohorts may assist in strengthening our conclusions. In addition, our study was cross sectional. Hence, we can only speculate that pupil function alterations predict the development of AD, but this must be tested in a longitudinal design, which is ongoing in the IRAP study [49]. Another limitation of our study is that it included only Caucasian subjects, which are the majority in the Israeli population. Hence, future studies including non-Caucasian individuals are required to expand the generalizability of our findings.

A third limitation concerns the ratio between subjects with and without AD family history. Most participants in our study had a confirmed AD family history, and they accounted for 67.2% of the study's participants. This number does not reflect the normal proportion of this condition in the population. This is attributed to the fact that our study participants are part of the IRAP cohort, which was formed as part of a longitudinal study [49]. Participants are required to undergo a battery of clinical testing including cognitive assessment, MRI and blood tests every several years. In this type of study design recruiting healthy subjects in more challenging.

To the best of our knowledge, this is the first attempt to identify focal changes in the rod- cone and melanopsin-mediated PLR in cognitively normal, asymptomatic participants at high risk for AD. Using

chromatic pupilloperimetry testing in a relatively large cohort and artificial intelligence tools, our study suggests that individuals at high risk to develop AD have specific changes, already in midlife, in the latency of PLR for focal dim red and blue light stimuli. Rod-circuits are specifically affected at the nasal retina whereas the cone-circuits are affected across the central retina, and melanopsin function remains unaffected at this early stage.

Methods

Study design and precipitants

Participants

The study was approved by the Sheba Medical Center and MHS institutional review board (IRB) committees and all participants signed an informed consent. The described research adhered to the tenets of the Declaration of Helsinki. Participants (N=301) are from the Israel Registry for Alzheimer's Prevention (IRAP) study, and all are members of the Maccabi Healthcare Services (MHS), the second largest HMO in Israel [49]. Briefly, participants were recruited through the MHS homepage and word of mouth. They were either offspring of AD patients (family history positive, FH+) or subjects with no parental history of AD (family history negative, FH-). Potential participants underwent questioning regarding their age, MHS membership, and parental dementia. Medical records of their parents were provided to the study team and a dementia questionnaire (DQ) was administered to determine the likely presence of AD in parents of potential study volunteers. The DQ is a validated, informant-based instrument [50]. The medical history, diagnostic workup and the DQ were reviewed by the study team to reach a probable AD diagnosis (according to NINCDS-ADRDA criteria)- or lack of, in parents of potential participants. In case of partial information about dementia type or with dementia other than AD, the potential participant was excluded from the study. Also excluded were offspring of parents with an AD onset before the age of 55 (which are assumed to have familial early onset AD). Siblings were excluded from the study for avoiding confounding results (the first eligible offspring who volunteered was included in the study). Detailed methods are provided in [49].

Brain MRI- Brain MRI was performed as part of the IRAP parent study. One hundred and twenty-seven participants had MRI done within the same year of chromatic pupilloperimetry testing and their data was included in the study. MRI scans were acquired on a three Tesla whole body MRI system (GE Signa HDxt, version 16 VO2) equipped with an eight-channel radio frequency head coil. The MRI scanning included T1-weighted imaging and T2-weighted-fluid-attenuated inversion recovery (T2-FLAIR) for clinical purposes[39]. The 3D T1-weighted images underwent the common processing pipeline for voxel-based morphometric analysis [51], using CAT12 [52] toolbox implemented in SPM12 software (https://www.fil.ion.ucl.ac.uk/spm/software/spm12/) in the MATLAB environment (The MathWorks, Inc., Natick, Massachusetts, United States)). Gray-matter, white-matter, and cerebrospinal fluid components were obtained to calculate the total intracranial volume in the native space. Gray matter and

Hippocampal volumes were extracted from the smoothed modulated and normalized images, and were entered into group comparisons adjusting for total intracranial volume.

Cognitive assessment- Subjects underwent cognitive assessment on the same day as chromatic pupilloperimetry testing. The neuropsychological tests included : Rey Auditory Verbal Learning test – immediate and delayed recall and recognition [53], Trail making tests A and B, the digit symbol substitution test [54] and the digit span tests forwards and backwards [55] The tests were all summarized into executive functions (EF), working memory (WM), and episodic memory (EM) domains. The scores of the neuropsychological tests were transformed into Z scores and averaged for each domain, as described in [49].

Ophthalmologic examination- Participants underwent a complete ophthalmologic examination on the same day as chromatic pupilloperimetry testing to exclude ocular pathologies including assessment of best-corrected visual acuity (BCVA), color vision (Farnsworth D15 test), pupillary reflexes, intraocular pressure (Goldmann applanation tonometry) and slit lamp bio-microscopy of the anterior and posterior segment, fundus examination and optical coherence tomography (OCT). Eyes with BCVA of 20/50 or lower, or any ocular pathology were excluded.

Only participants for whom both eyes were eligible for the study were included, a total of 186 patients and 372 eyes (see Figure 3). Sixty-one of them were FH- and 125 were FH+.

Chromatic pupilloperimetry

On the same day of cognitive and ophthalmic assessments, each participant underwent chromatic pupilloperimetry testing in both eyes, resulting in a sum of 372 eyes (250 eyes were FH+ and 122 were FH-).

Chromatic pupilloperimetry testing was performed as previously described [37]. Briefly, the device is comprised of a Ganzfeld dome apparatus with 76 LEDs (2 mm^2 diameter), an infrared camera and a fixation light. Each eye was tested separately, and non-tested eye was occluded to prevent PLR due to light perception in the contralateral eye.

Cone- and rod- mediated PLR were recorded using red (624nm, 1000 cd/m^2) and dim blue (485nm, 170 cd/m^2) light stimuli, respectively. Light stimuli were presented from individual LEDs, illuminating 54 different spots in the retina for one second, and pupil diameter was captured for 4 seconds by a computerized infrared high-resolution video camera (Figure 4a-c).

Melanopsin mediated PLR was recorded using bright (6000 cd/m^2) red (624nm) and blue (485 nm) light stimuli, that were presented at two central and two peripheral retinal locations, for 8 seconds, and pupil diameter was captured for 16 seconds (Figure 4d-f).

Test targets in which the subject blinked during the first 2.5 seconds following light onset were automatically excluded and the targets were automatically retested at the end of the sequence.

Seventeen PLR parameters from both the contraction and dilatation phase were calculated and analyzed for both eyes of each participant. These include pupil contraction and dilation amplitude, velocity, acceleration, and latencies (Supplementary Method 1).

Each one of these parameters was calculated for the PLR response for red, dim and bright blue -light stimuli in each test point resulting in a total of 34 independent parameters for each one of the 54 test point locations for red and dim blue light, and 34 independent parameters for each of the 4 test point locations for bright blue light.

Machine Learning analysis

Using the Chromatic Pupilloperimeter we analyzed the significance of each of the PLR parameters for each of the test point locations, in order to classify participants to either having or not having a family history of AD.

Each parameter produced either 54 or 4 independent features for the PLR parameter measured at the different test targets of the visual field (VF). Our goal was to estimate and compare the predictive accuracy of the different parameters.

We used the AdaBoost algorithm, a widely used boosting algorithm, with a solid theoretical background [56], for training multiple classifiers. Each classifier received a distinct set of features corresponding to a single PLR parameter. The process was repeated for each eye independently.

For each eye, 17 models were trained based on the 17 PLR parameters extracted using red light, 17 models were trained based on the 17 PLR parameters extracted using dim blue light, 17 models trained based on the 17 PLR parameters extracted using bright blue light, and another 17 models trained based on the 17 PLR parameters extracted using bright red light resulting in a total of 68 X (2 eyes) = 136 different models. We note that a classifier may be trained using a combination of inter parameter features.

Missing data, which were 0.76% from the data, were imputed [5758]. Imputation was performed using the mean substitution strategy that assigns the overall respondent mean to all missing responses and is the deterministic degenerate form of the linear function with no auxiliary variables. All features were rescaled using min-max normalization to a range of [0,1].

Discrimination performance of the classification model was measured by the Area Under the Receiver Operating Curve (AUC-ROC).

Statistical analysis

Comparisons between FH+ and FH- groups were performed using chi-square tests for sex category and using a t-test for years of education. General linear model was used to compare MRI gray matter and hippocampal volume adjusting for total intracranial volume (Table 1). For comparisons of the cognitive domains between FH+ and FH- groups we used MANOVA. We then adjusted for age, sex, and education using ANCOVAs. Raw scores of each cognitive test are presented in Supplementary Table 1. Analysis was done with SPSS v. 20 (IBM, USA).

To assess the confidence interval for the AUC-ROC, we used non-parametric resampling [59] The general algorithm for a non-parametric bootstrap, applied here, was comprised of the following: 1. Sample *n* observations randomly with replacement from the 186 samples (*n* = 186) to obtain a bootstrap dataset. Sampling was performed in a stratified fashion. 2. Train a classifier using the bootstrap version of the data, test it on the observations that are not part of the bootstrap dataset, to conclude an AUC-ROC measure. 3. Repeat steps 1. and 2. on 2000 replicates, as recommended when calculating CI using bootstrapping [60], to obtain an estimate of the confidence interval.

Declarations

Author contributions:

Conceptualization: YLB, IS, YR; Experimental design: YLB, IS, YR, MSB, RRS; Data collection: IS, ISG, AL; Data analysis: YLB, IS, YF, AL, MM, IS; Manuscript preparation: YLB, IS, Manuscript review and editing: YLB, IS, AW, AL, MM, MSB, RRS, YR,

Data availability:

The data that support the findings of this study are available upon a reasonable request from the corresponding author [YR]. The data are not publicly available due to them containing information that could compromise research participant privacy.

Competing interests:

IS and YR have patents and patent application regarding chromatic pupilloperimetry methods and device, handled by the Sheba Medical Center. All other authors declare no competing interests.

Funding: This study was supported by the Israel Science Foundation (ISF, grant ID: 1845/16) to YR, MSB, RRS.

References

1. Wimo, A. *et al.* The worldwide economic impact of dementia 2010. Alzheimers Dement **9**, 1-11.e3 (2013).

2. Dunn, B., Stein, P. & Cavazzoni, P. Approval of Aducanumab for Alzheimer Disease-The FDA's Perspective. JAMA Intern. Med. **181**, 1276–1278 (2021).
3. Hsu, D. & Marshall, G. A. Primary and secondary prevention trials in alzheimer disease: looking back, moving forward. Curr. Alzheimer Res. **14**, 426–440 (2017).
4. Cummings, J. L., Doody, R. & Clark, C. Disease-modifying therapies for Alzheimer disease: challenges to early intervention. Neurology **69**, 1622–1634 (2007).
5. van Duijn, C. M. *et al.* Familial aggregation of Alzheimer's disease and related disorders: a collaborative re-analysis of case-control studies. Int. J. Epidemiol. **20 Suppl 2**, S13-20 (1991).
6. Payami, H. *et al.* A prospective study of cognitive health in the elderly (Oregon Brain Aging Study): effects of family history and apolipoprotein E genotype. Am. J. Hum. Genet. **60**, 948–956 (1997).
7. Green, R. C. *et al.* Risk of dementia among white and African American relatives of patients with Alzheimer disease. JAMA **287**, 329–336 (2002).
8. Bendlin, B. B. *et al.* Midlife predictors of Alzheimer's disease. Maturitas **65**, 131–137 (2010).
9. Scarabino, D., Gambina, G., Broggio, E., Pelliccia, F. & Corbo, R. M. Influence of family history of dementia in the development and progression of late-onset Alzheimer's disease. Am. J. Med. Genet. B Neuropsychiatr. Genet. **171B**, 250–256 (2016).
10. Snyder, P. J. *et al.* Nonvascular retinal imaging markers of preclinical Alzheimer's disease. Alzheimers Dement (Amst) **4**, 169–178 (2016).
11. van de Kreeke, J. A. *et al.* Retinal layer thickness in preclinical Alzheimer's disease. Acta Ophthalmol. **97**, 798–804 (2019).
12. Alber, J. *et al.* Developing retinal biomarkers for the earliest stages of Alzheimer's disease: What we know, what we don't, and how to move forward. Alzheimers Dement **16**, 229–243 (2020).
13. La Morgia, C. *et al.* Melanopsin retinal ganglion cell loss in Alzheimer disease. Ann. Neurol. **79**, 90–109 (2016).
14. Hall, C. A. & Chilcott, R. P. Eyeing up the future of the pupillary light reflex in neurodiagnostics. Diagnostics (Basel) **8**, 19 (2018).
15. Chougule, P. S., Najjar, R. P., Finkelstein, M. T., Kandiah, N. & Milea, D. Light-Induced Pupillary Responses in Alzheimer's Disease. Front. Neurol. **10**, 360 (2019).
16. Prettyman, R., Bitsios, P. & Szabadi, E. Altered pupillary size and darkness and light reflexes in Alzheimer's disease. J. Neurol. Neurosurg. Psychiatr. **62**, 665–668 (1997).
17. Frost, S. *et al.* Pupil response biomarkers for early detection and monitoring of Alzheimer's disease. Curr. Alzheimer Res. **10**, 931–939 (2013).
18. Ferrario, E. *et al.* Is videopupillography useful in the diagnosis of Alzheimer's disease? Neurology **50**, 642–644 (1998).
19. Bittner, D. M., Wieseler, I., Wilhelm, H., Riepe, M. W. & Müller, N. G. Repetitive pupil light reflex: potential marker in Alzheimer's disease? J Alzheimers Dis **42**, 1469–1477 (2014).

20. Granholm, E. *et al.* Tropicamide effects on pupil size and pupillary light reflexes in Alzheimer's and Parkinson's disease. Int. J. Psychophysiol. **47**, 95–115 (2003).
21. Fotiou, D. F. *et al.* Pupil reaction to light in Alzheimer's disease: evaluation of pupil size changes and mobility. Aging Clin. Exp. Res. **19**, 364–371 (2007).
22. Fotiou, D. F. *et al.* Cholinergic deficiency in Alzheimer's and Parkinson's disease: evaluation with pupillometry. Int. J. Psychophysiol. **73**, 143–149 (2009).
23. Frost, S. *et al.* Evaluation of cholinergic deficiency in preclinical alzheimer's disease using pupillometry. *J. Ophthalmol.* 2017, 7935406 (2017).
24. Frost, S. M. *et al.* Pupil response biomarkers distinguish amyloid precursor protein mutation carriers from non-carriers. Curr. Alzheimer Res. **10**, 790–796 (2013).
25. Fotiou, D., Kaltsatou, A., Tsiptsios, D. & Nakou, M. Evaluation of the cholinergic hypothesis in Alzheimer's disease with neuropsychological methods. Aging Clin. Exp. Res. **27**, 727–733 (2015).
26. Van Stavern, G. P., Bei, L., Shui, Y.-B., Huecker, J. & Gordon, M. Pupillary light reaction in preclinical Alzheimer's disease subjects compared with normal ageing controls. Br. J. Ophthalmol. **103**, 971–975 (2019).
27. Kardon, R. *et al.* Chromatic pupil responses: preferential activation of the melanopsin-mediated versus outer photoreceptor-mediated pupil light reflex. Ophthalmology **116**, 1564–1573 (2009).
28. Park, J. C. *et al.* Toward a clinical protocol for assessing rod, cone, and melanopsin contributions to the human pupil response. Invest. Ophthalmol. Vis. Sci. **52**, 6624–6635 (2011).
29. Gooley, J. J. *et al.* Melanopsin and rod-cone photoreceptors play different roles in mediating pupillary light responses during exposure to continuous light in humans. J. Neurosci. **32**, 14242–14253 (2012).
30. Rukmini, A. V., Milea, D. & Gooley, J. J. Chromatic pupillometry methods for assessing photoreceptor health in retinal and optic nerve diseases. Front. Neurol. **10**, 76 (2019).
31. Park, J. C. & McAnany, J. J. Effect of stimulus size and luminance on the rod-, cone-, and melanopsin-mediated pupillary light reflex. J. Vis. **15**, 13 (2015).
32. Oh, A. J. *et al.* Pupillometry evaluation of melanopsin retinal ganglion cell function and sleep-wake activity in pre-symptomatic Alzheimer's disease. PLoS ONE **14**, e0226197 (2019).
33. Romagnoli, M. *et al.* Chromatic pupillometry findings in alzheimer's disease. Front. Neurosci. **14**, 780 (2020).
34. Haj Yahia, S. *et al.* Effect of Stimulus Intensity and Visual Field Location on Rod- and Cone-Mediated Pupil Response to Focal Light Stimuli. Invest. Ophthalmol. Vis. Sci. **59**, 6027–6035 (2018).
35. Chibel, R. *et al.* Chromatic Multifocal Pupillometer for Objective Perimetry and Diagnosis of Patients with Retinitis Pigmentosa. Ophthalmology **123**, 1898–1911 (2016).
36. Ben Ner, D. *et al.* Chromatic pupilloperimetry for objective diagnosis of Best vitelliform macular dystrophy. Clin. Ophthalmol. **13**, 465–475 (2019).

37. Sher, I. *et al.* Chromatic pupilloperimetry measures correlate with visual acuity and visual field defects in retinitis pigmentosa patients. Transl. Vis. Sci. Technol. **9**, 10 (2020).
38. Skaat, A. *et al.* Pupillometer-based objective chromatic perimetry in normal eyes and patients with retinal photoreceptor dystrophies. Invest. Ophthalmol. Vis. Sci. **54**, 2761–2770 (2013).
39. Bartus, R. T., Dean, R. L., Beer, B. & Lippa, A. S. The cholinergic hypothesis of geriatric memory dysfunction. Science **217**, 408–414 (1982).
40. Van Beek, A. H. E. A. & Claassen, J. A. H. R. The cerebrovascular role of the cholinergic neural system in Alzheimer's disease. Behav. Brain Res. **221**, 537–542 (2011).
41. Ferreira-Vieira, T. H., Guimaraes, I. M., Silva, F. R. & Ribeiro, F. M. Alzheimer's disease: Targeting the Cholinergic System. Curr. Neuropharmacol. **14**, 101–115 (2016).
42. Scinto, L. F. *et al.* Focal pathology in the Edinger-Westphal nucleus explains pupillary hypersensitivity in Alzheimer's disease. Acta Neuropathol. **97**, 557–564 (1999).
43. Scinto, L. F. *et al.* Selective cell loss in Edinger-Westphal in asymptomatic elders and Alzheimer's patients. Neurobiol. Aging **22**, 729–736 (2001).
44. Hultborn, H., Mori, K. & Tsukahara, N. The neuronal pathway subserving the pupillary light reflex. Brain Res. **159**, 255–267 (1978).
45. Fotiou, F., Fountoulakis, K. N., Tsolaki, M., Goulas, A. & Palikaras, A. Changes in pupil reaction to light in Alzheimer's disease patients: a preliminary report. Int. J. Psychophysiol. **37**, 111–120 (2000).
46. Tales, A. *et al.* The pupillary light reflex in aging and Alzheimer's disease. Aging (Milano) **13**, 473–478 (2001).
47. McAnany, J. J. *et al.* Rod pathway and cone pathway retinal dysfunction in the 5xFAD mouse model of Alzheimer's disease. Sci. Rep. **11**, 4824 (2021).
48. Do, K. V. *et al.* Elovanoids counteract oligomeric β-amyloid-induced gene expression and protect photoreceptors. Proc Natl Acad Sci USA **116**, 24317–24325 (2019).
49. Ravona-Springer, R. *et al.* The israel registry for alzheimer's prevention (IRAP) study: design and baseline characteristics. J Alzheimers Dis **78**, 777–788 (2020).
50. Ellis, R. J. *et al.* Diagnostic validity of the dementia questionnaire for Alzheimer disease. Arch. Neurol. **55**, 360–365 (1998).
51. Ashburner, J. & Friston, K. J. Voxel-based morphometry--the methods. Neuroimage **11**, 805–821 (2000).
52. Gaser, C. & Dahnke, R. CAT-A Computational Anatomy Toolbox for the Analysis of Structural MRI Data. (2016).
53. Chelune, G. J. & Baer, R. A. Developmental norms for the Wisconsin Card Sorting test. J. Clin. Exp. Neuropsychol. **8**, 219–228 (1986).
54. Wechsler, D. *Wechsler adult intelligence scale-revised*. 1–156 (Psychological Corporation, 1981).
55. Elwood, R. W. The Wechsler Memory Scale-Revised: psychometric characteristics and clinical application. Neuropsychol. Rev. **2**, 179–201 (1991).

56. Freund, Y. & Schapire, R. E. A Decision-Theoretic Generalization of On-Line Learning and an Application to Boosting. Journal of Computer and System Sciences **55**, 119–139 (1997).
57. kalton, G. & Kasprzyk, D. The treatment of missing survey data. Survey methodology **12**, 1–16 (1986).
58. Kalton, G. & Kasprzyk, D. Imputing for missing survey responses. American Statistical Association **22**, 31 (1982).
59. DiCiccio, T. J. *et al.* Bootstrap confidence intervalsCommentCommentCommentCommentRejoinder. Stat. Sci. **11**, 189–228 (1996).
60. Carpenter, J. & Bithell, J. Bootstrap confidence intervals: when, which, what? A practical guide for medical statisticians. Stat. Med. **19**, 1141–1164 (2000).

Figures

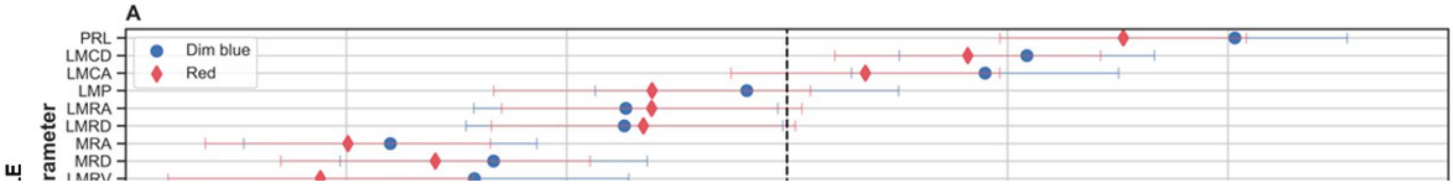

Figure 1

The mean Area Under the Receiver's Operating Curve (AUC-ROC) for each PLR parameter for dim red (red diamond) and blue (blue circle) light stimuli in the left (**a**) and right (**b**) eyes were measured using the bootstrapping process (depicted in Figure 6). Error bars represent the Standard Deviation for each parameter. The black dashed lines highlight the cutoff of AUC-ROC=0.7.

Figure 2

The relative weight given by the machine-learning model to each one of the 54 retinal test-targets for Pupil Response Latency (PRL) in the left (a,c) and right eye (b,d) for dim blue (a, b, B_PRL) and dim red light stimuli (c,d , R_PRL). The weights were averaged over the 2000 trials that were used to produce the 95% CI, as depicted in Figure 5. Color-coding indicates higher weights in darker colors.

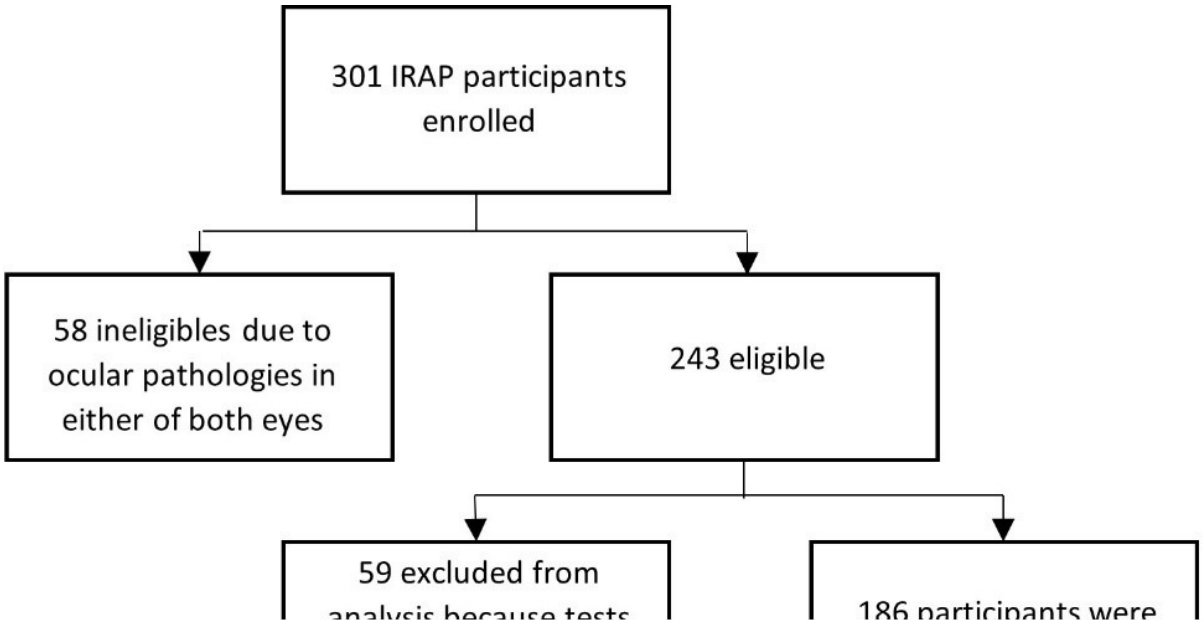

Figure 3

Flow chart of the study recruitment

Figure 4

Chromatic pupilloperimetry light stimulus presentation and PLR waveform. The chromatic pupilloperimetry test included 54 test locations in a pattern resembling the Humphrey perimetry 24-2 visual field test. First, the red-light stimuli were presented for 1 second at the indicated sequence (1-54, a). Next, dim blue light stimuli were presented for 1 second (55-108, **b**). Finally, Bright red-light stimuli were presented for 8 seconds at two central and two peripheral (**d**) retinal location followed by bright blue stimuli at the same sequence (**e**). The right eye test pattern is presented in panels a-b and d-e. **e- c,** f - a schematic presentation of transient (c) and sustained **(**f) PLR wave forms obtained in response to dim (c) and bright (f) red and blue light stimuli. Demonstration of the Pupil Response Latency (PRL) is indicated with arrows (c, f).

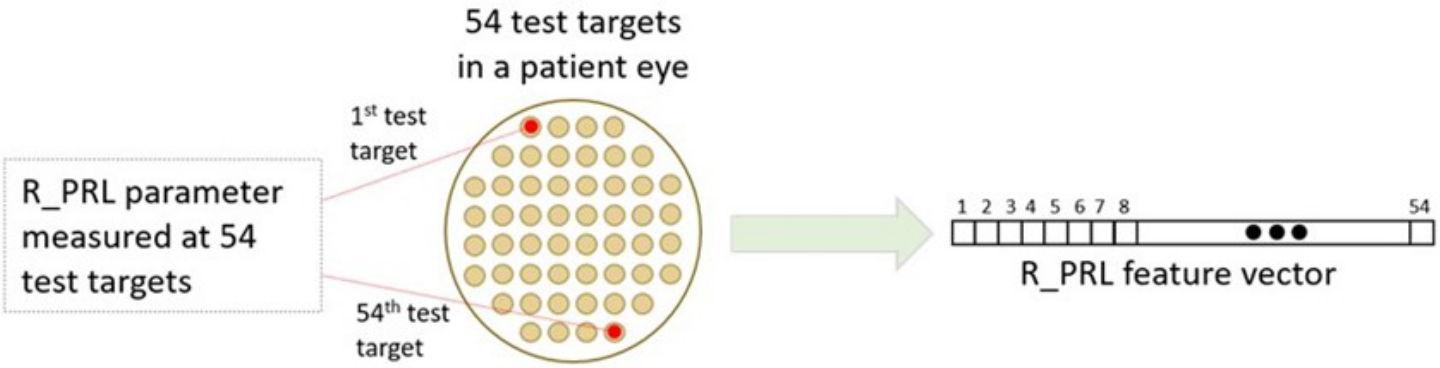

Figure 5

An illustration of a feature vector extraction process from a participant's chromatic pupilloperimetry test. Here a vector for the Pupil Response Latency of a red stimulus (R_PRL), measured in 54 test targets, was generated. The process was repeated per both eyes of each patient.

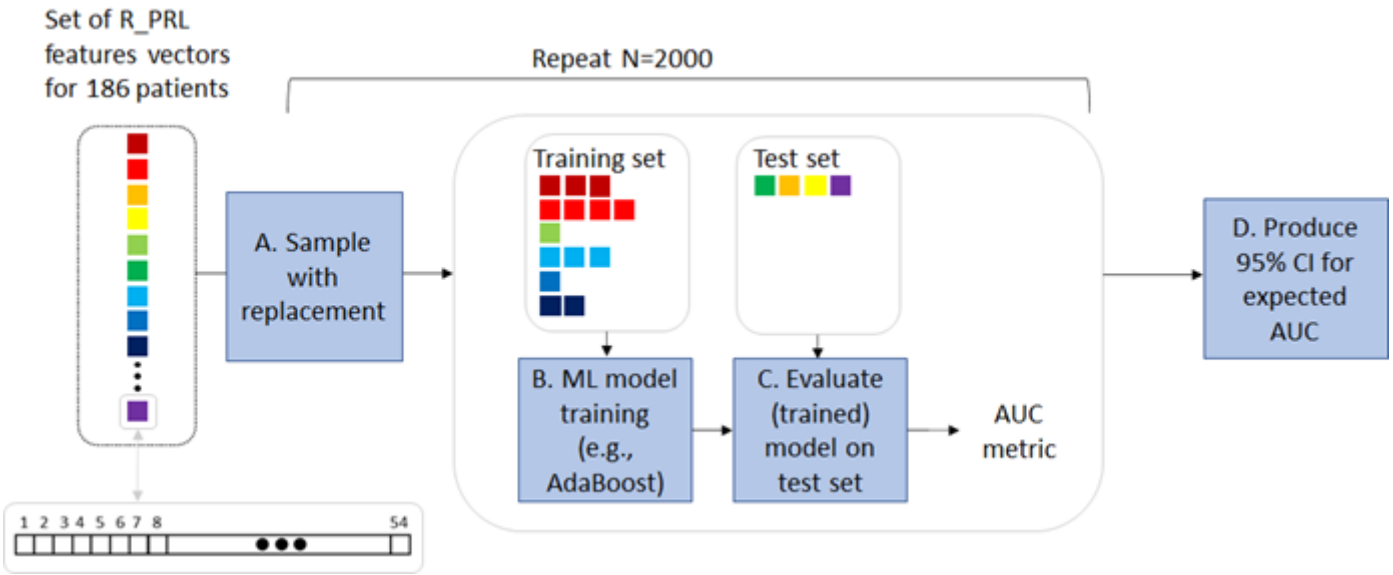

Figure 6

An illustration of producing a confidence interval (CI) for a single PLR parameter (in this case, R_PRL). Given the full set of samples, a training set was created by sampling with replacement, whereas the test set was comprised of all the samples that were not picked in the training set. The model was evaluated on the test set (average size of 88 distinct samples) using the AUC-ROC the metric. The process was repeated N=2000 times to infer a 95% CI. R_PRL: Pupil Reflex Latency induced by red light, CI: Confidence Interval, AUC-ROC: Area Under the Receiver's Operating Curve.

Supplementary Files

This is a list of supplementary files associated with this preprint. Click to download.

- Supplementary.docx